THE RADIO FREQUENCY FRAGMENT SEPARATOR: A TIME-OF-FLIGHT FILTER FOR FAST FRAGMENTATION BEAMS*

T. Baumann, D. Bazin, T. N. Ginter, E. Kwan, J. Pereira, C. S. Sumithrarachchi
NSCL, Michigan State University, East Lansing, MI 48824, USA

Abstract

Rare isotope beams produced by fragmentation of fast heavy-ion beams are commonly separated using a combination of magnetic rigidity selection (mass-to-charge ratio) and energy-loss selection (largely dependent on proton number) using magnetic fragment separators. This method offers isotopic selection of the fragment of interest, however, the purity that can be achieved is often not sufficient for neutron-deficient isotopes (towards the proton drip line) where much more abundant isotopes closer to stability can not be separated out. A separation by time-of-flight can clean things up. The Radio Frequency Fragment Separator deflects isotopes based on their phase relative to the cyclotron RF using a transverse RF field, effectively separating by time-of-flight. This method is in use for the production of neutron deficient rare isotope beams at NSCL.

INTRODUCTION

Rare isotope beams that are produced in fast fragmentation reactions give access to a large range of radioactive isotopes for in-beam nuclear physics experiments, from the most neutron-rich isotopes that have ever been observed up to the proton drip line for many elements. Many experiments require beams of high purity, and for neutron deficient rare isotopes in particular this is often difficult to achieve using magnetic fragment separators. The problem originates from a low momentum tail produced in the fragmentation process, which occurs for projectile energies between 50 MeV/u and 200 MeV/u. This causes much more abundant fragments that are closer to stability to spill into the acceptance window of the desired isotope.

The Radio Frequency Fragment Separator (RFFS) [1] at the National Superconducting Cyclotron Laboratory (NSCL) was built to address this problem. It uses the time structure of the particle beams that are accelerated by the coupled cyclotrons to deflect unwanted fragments based on the difference in velocity. In this paper we will give a brief summary of how the RFFS functions and focus on two recent experiments that give a real world view of its performance.

Function of the RF Fragment Separator

The RFFS is basically the combination of an RF driven electric deflector that diverts the particle beam vertically at a specified phase of the cyclotron RF, and a set of slits that blocks unwanted particles. The detailed parameters of the RFFS are given in Ref. [1]. Figure 1 shows a side view of the RF cavity.

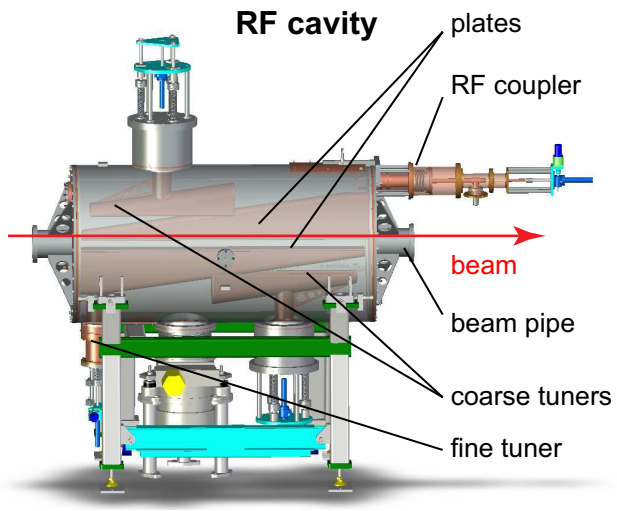

Figure 1: Side view of the RFFS cavity.

The length of the electrodes is 1.5 m which covers approximately 140° of the phase with typical beam velocities of around $0.4c$ and the given cyclotron frequency of about 25 MHz. The vertical gap between the electrodes is 5 cm, and the nominal operating peak voltage is 100 kV.

Following the RF deflector, the particle beam is focused on a pair of vertical slits in the RFFS focal plane box. These slits are adjustable in order to block the unwanted parts of the beam depending on their vertical position. The RFFS focal plane box also contains detectors to perform the particle identification. A pair of parallel plate avalanche counters (PPACs) gives position and angle information, a 250 μm plastic scintillator timing, and a stack of Si PIN detectors energy-loss information.

Under normal operating conditions, the phase of the RFFS is set such that the fragment of interest receives the maximum deflection, and unwanted fragments that are less deflected are blocked by the slits. The deflected beam position is then corrected by a pair of steering magnets before reaching the experimental setup. This method has the advantage that in case of a failure of the RF deflector, the possibly highly intense unwanted beam will still be blocked by the slits, minimizing the risk of damaging rate sensitive detectors.

EXPERIMENTAL EXAMPLES

The RFFS is one of the tools that are available at NSCL to provide rare isotope beams to facility users. Two recent experiments will serve as examples of neutron deficient rare isotope beams that benefited from the use of the RFFS.

* Work supported by NSF grants

ISBN 978-3-95450-128-1

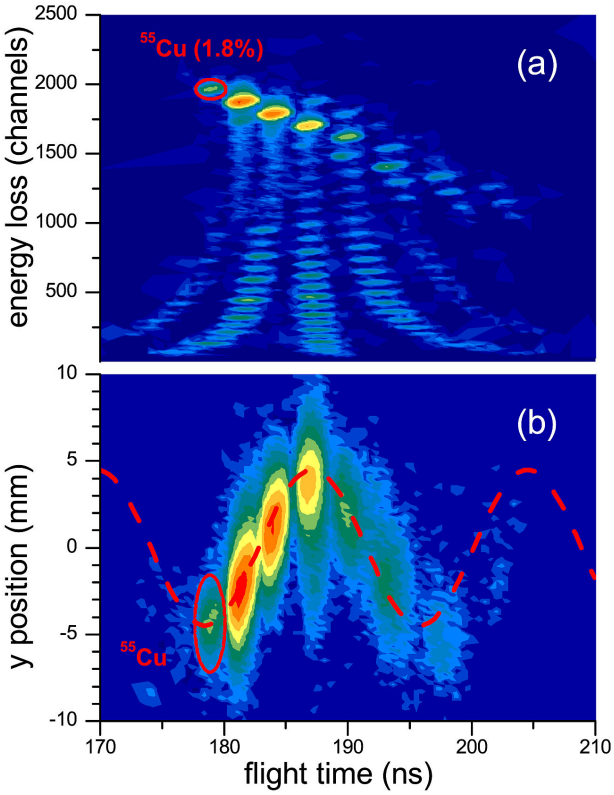

Figure 2: Particle identification plots as recorded in the RFFS focal plane. Panel (a) shows an energy-loss versus time-of-flight plot. The red ellipse indicates the location of ^{55}Cu. Panel (b) shows the vertical position of the beam with respect to the beam axis folowing the RFFS. The horizontal scale is identical to panel (a). The red dashed line is a sine wave approximating the radio frequency.

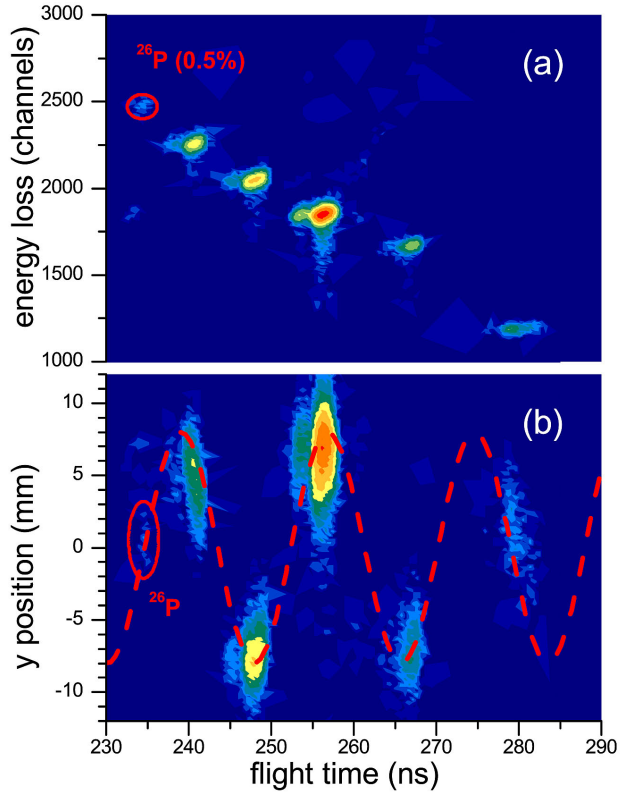

Figure 3: Panel (a) and (b) show the same spectra as in Fig. 2 but in this case for ^{26}P.

Neutron Deficient ^{55}Cu and ^{26}P

^{55}Cu is the lightest of the Cu isotopes, located at the proton drip line, and was only discovered in 1987 [2, 3]. Beam physicists at the NSCL chose ^{58}Ni at 160 MeV/u as a primary beam to produce ^{55}Cu by projectile fragmentation in a Be target. The rare isotope beam was separated from the unreacted primary beam and other fragments using the A1900 fragment separator [4]. The fragment separator selects isotopes based on their magnetic rigidity. A wedge-shaped aluminum degrader at the dispersive mid-plane of the A1900 further enables isotopic selection. The beam energy of the ^{55}Cu after the fragment separator was about 100 MeV/u. Fragments with similar mass-to-charge ratio close to ^{55}Cu, namely ^{54}Ni, ^{53}Co, ^{52}Fe, ^{51}Mn etc., were strong contaminants (see Fig. 2). These isotopes have a much higher production yield compared to ^{55}Cu since they are closer to the valley of stability. Because of their low momentum tails they could not be discriminated using the A1900 fragment separator alone. This resulted in a beam with less that 2% purity. For this reason the RFFS was employed to further purify the rare isotope beam.

The isotope ^{26}P is also a drip line nucleus and was discovered in 1983 [5, 6]. For the production of ^{26}P an ^{36}Ar beam of 150 MeV/u was used, which was fragmented on a Be target. As in the previous example, an aluminum wedge was employed to further purify the beam, but a purity of only 0.5% was achieved (see Fig. 3). Isotopes with similar mass-to-charge ratio as ^{26}P, i.e. ^{25}Si, ^{24}Al, ^{23}Mg etc., were the main contaminants. The beam energy of the ^{26}P beam was about 55 MeV/u, which makes it almost 25% slower than the ^{55}Cu beam.

Beam Selection with the RFFS

There are three adjustments of the RFFS that determine which isotopes are blocked: the RF phase, the slit setting, and the RF voltage. The voltage of the RFFS is usually set to 90 kV and not further adjusted.

Which part of the beam cocktail gets blocked by the slits depends on the phase of the isotope relative to the fragment of interest. The phase is determined by the time offset between the fragment of interest and the contaminants, which itself depends on the velocity ratio and the flight path from the production target to the RFFS.

In the two described examples, the fragment of interest is the most proton rich isotope in the mix, which means that it is the fastest of the isotopes. In the case of ^{55}Cu, the fragment energy and therefore velocity was high such that the strongest contaminants all followed the fragment

ISBN 978-3-95450-128-1

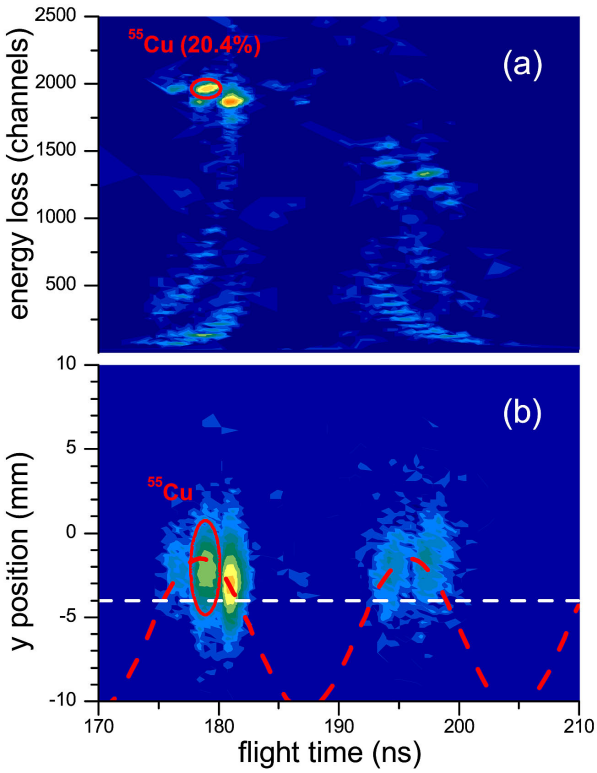

Figure 4: Panels (a) and (b) again show the same spectra as in previous figures, but this time parts of the beam are blocked by the RFFS vertical focal plane slits. The white dashed line shows the approximate position of the slits. In this case for ^{55}Cu, the contaminant ^{54}Ni can not be completely blocked due to it's proximity in phase.

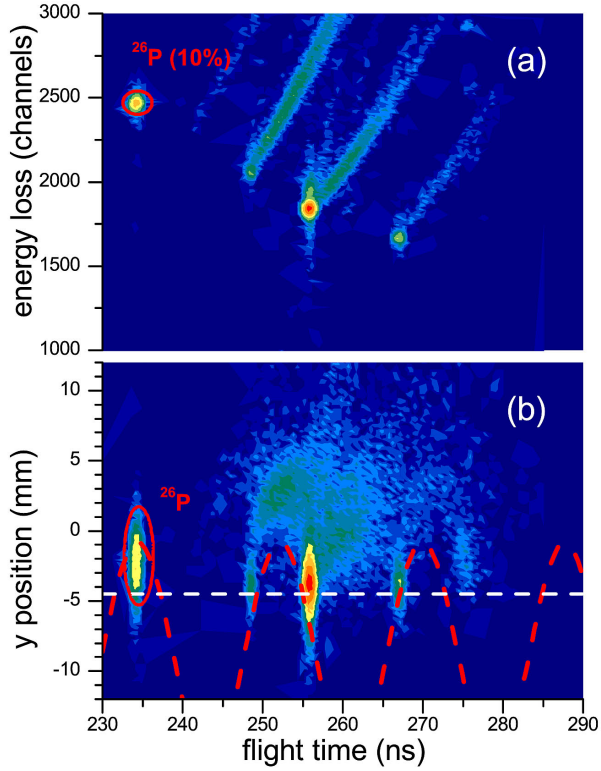

Figure 5: Particle identification plots for the ^{26}P setting with inserted RFFS focal plane slits, the approximate position is indicated by the white dashed line in panel (b). ^{23}Mg has a phase shift close to one RF period, so it can not be completely blocked.

of interest within the first 180° of phase. All but the direct neighbor could be blocked by the slits. The purity of the ^{55}Cu beam was improved to over 20% (see Fig. 4).

In the case of ^{26}P, the fragment energy was much lower, which caused the contaminants to be spread out over a larger phase of over 360°. There are only two ways to resolve such a situation, one is to change the location of the RFFS in the beam line, and the other is to chose a different beam energy. Since the location of the device in the beam line is fixed, the only possible adjustment is to change the energy of the fragment beam. However, to make a significant enough change in phase requires a drastic change in energy. In this case such a change was not possible due to the limitations in the fragment production and the requirements of the experiment. Still a purity of 10% was achieved for the ^{26}P beam after optimizing phase and slit settings (see Fig. 5).

CONCLUSION

The RFFS is a tool to produce rare isotope beams of high purity at the NSCL's Coupled Cyclotron Facility. It was designed to enable the studies of rare neutron deficient isotopes. Under optimal conditions it can improve the purity of the rare isotope beam by a factor 100 to 1000, compared to the beam produced by the A1900 fragment separator alone. In many experiments the conditions are not optimal for the RFFS filtering due to restrictions of usable beam energy, either because a specific beam energy is needed for the experiment, or because the fragment of interest can only be produced at a reasonable rate at a given energy. But even in these cases a purification of a factor of 10 to 20 can be achieved with careful planning and optimization of the RFFS settings.

REFERENCES

[1] D. Bazin, V. Andreev, A. Becerril, M. Doléans, P. F. Mantica, J. Ottarson, H. Schatz, J. B. Stoker, and J. Vincent, Nucl. Inst. and Meth. Phys. Res. A 606, 314–319 (2009)

[2] K. Garofali, R. Robinson, and M. Thoennessen, At. Data Nucl. Data Tables 98, 356–372 (2012)

[3] F. Pougheon, et al., Z. Phys. A 327 17–24 (1987)

[4] A. Stolz, T. Baumann, T. N. Ginter, D. J. Morrissey, M. Portillo, B. M. Sherrill, M. Steiner, and J. W. Stetson, Nucl. Inst. and Meth. Phys. Res. B 241, 858–861 (2005)

[5] M. D. Cable, J. Honkanen, R. F. Parry, S. H. Zhou, Z. Y. Zhou, and J. Cerny, Phys. Lett. B 123, 25–28 (1983)

[6] M. Thoennessen, At. Data Nucl. Data Tables 98, 933–959 (2012)

ISBN 978-3-95450-128-1